A SEARCH FOR REGIONAL SIGNATURES OF SPACE WEATHERING ON MERCURY. Deborah L. Domingue (domingue@psi.edu)[1], Patrick N. Peplowski[2], Larry R. Nittler[3], Mario D'Amore[4], Jörn Helbert[4], David Schriver[5], Pavel M. Trávníček[6], Scott L. Murchie[2], Brett W. Denevi[2], Faith Vilas[1], Shoshana Z. Weider[3], Richard D. Starr[7], Ellen J. Crapster-Pregont[8] and Denton S. Ebel[8]. [1]Planetary Science Institute, Tucson AZ, 85719, USA. [2]Johns Hopkins University Applied Physics Laboratory, Laurel MD, 20723, USA. [3]Department of Terrestrial Magnetism, Carnegie Institution of Washington, Washington, DC 20015, USA. [4]Institute for Planetary Research, DLR, 12489 Berlin, Germany. [5]Institute of Geophysics and Planetary Physics, University of California, Los Angeles, CA 90024, USA. [6]Space Sciences Laboratory, University of California, Berkeley, CA 90704, USA. [7]Physics Department, The Catholic University of America, Washington, DC 20064, USA. [8]Dept. of Earth and Planetary Sciences, American Museum of Natural History, New York, NY 10024, USA.

Space Weathering. Mercury's surface is modified by a set of space weathering processes that fall under two main categories: (1) meteoroid and micrometeoroid bombardment and (2) solar wind and photon irradiation. A third, less prominent category, thermal cycling, may have a more substantial role at Mercury compared with the Moon or most asteroids due to the former's proximity to the Sun. The majority of our understanding of these processes comes from comparisons of lunar and asteroid samples (including meteorites) with remote sensing observations of their parent bodies. In this study we examine possible spatial variations in Mercury's space weathering processes and their potential signature(s) in the remote sensing observations from the MErcury Surface, Space ENvironment, GEochemistry, and Ranging (MESSENGER) spacecraft in orbit around Mercury.

MESSENGER's payload includes the Mercury Atmospheric and Surface Composition Spectrometer (MASCS), the Mercury Dual Imaging System (MDIS) that includes a wide-angle camera and an 11-color filter wheel, as well as two spectrometers dedicated to determining Mercury's elemental chemistry, a Gamma-Ray and Neutron Spectrometer (GRNS) and an X-Ray Spectrometer (XRS). Space weathering affects the spectral signatures measured with MASCS and MDIS by darkening (lowering the albedo), reducing spectral contrast (broadening and diminishing the strength of absorption features), creating spectral "reddening" (increasing the spectral slope) at visible and near-infrared (VNIR) wavelengths, and creating spectral "bluing" (decreasing the spectral slope) at ultraviolet wavelengths [1]. Space weathering processes also have a role in the removal, mobilization, and redistribution of volatile species (including alkali metals) within the regolith [2], which may affect the abundance and distribution of elements observed by the GRNS and XRS.

Environmental Factors. The three environmental factors that most strongly influence the space weathering processes are micrometeoroid flux, surface temperature, and the flux of solar wind and magnetospheric particles to the surface. These factors are influenced by Mercury's proximity to the Sun and its internally generated magnetic field. For example, higher micrometeoroid fluxes result in higher glass and nanophase iron ($npFe^0$) production. Higher surface ion fluxes increase lattice damage sites (thus increasing volatile adsorption efficiency), in addition to increasing the $npFe^0$ production. Higher temperatures accelerate melting and radiation damage propagation and introduce structural changes [3,4].

Earth's micrometeoroid flux is anisotropic [5,6,7]. Monte Carlo simulations of radar observations of meteoroid flux show that the dominant contribution (~70% of the total particle flux) is centered about the apex to Earth's motion, with two other sources, sunward and anti-sunward, providing the remaining ~30% of the flux [7]. These Earth-based studies demonstrate that the micrometeoroid flux is not isotropic at 1AU, but it is unclear how this pattern might map to Mercury's location.

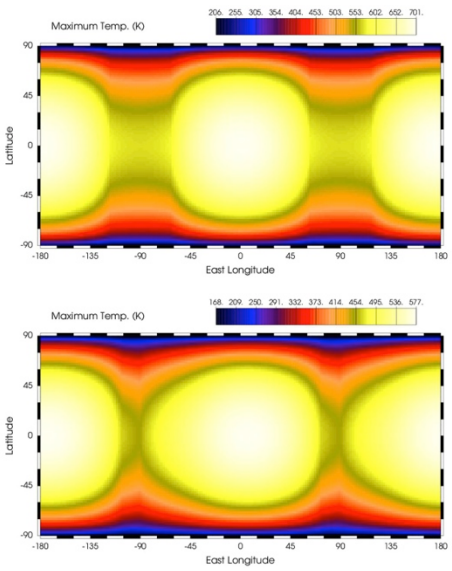

Fig. 1. Map of the maximum temperature experienced at Mer-Mercury's surface (top) and at 7 cm depth (bottom) derived from the formalism of Vasavada et al. [9], without account for topography. Images courtesy of David Paige (UCLA).

The maximum surface temperatures experienced by Mercury are shown in map view in Fig. 1 from the formulation of Vasavada et al. [9]. Mercury's hot poles (regions of maximum temperature) are centered at the equator at 0° and 180° E longitude, with cold poles (minimum temperature) centered at 90° and 270° E longitude. Also displayed in Fig. 1 are the maximum temperatures experienced at a depth of 7 cm depth, approximately the sampling depth of gamma-ray spectroscopy. If temperature drives the efficiency of most space weathering processes, then the signatures in the remote sensing data should display patterns similar to those in

these maps. From these temperature maps, Mercury's surface was divided into four longitude sectors, two hot pole (0° ± 30° and 180° ±30°E) and two cold pole (90° ± 30° and 270° ± 30°E) regions. Data from the MDIS, MASCS, XRS, and GRNS instruments were organized into these temperature-based longitude divisions.

The flux of ions and electrons to Mercury's surface varies with both the sunward versus anti-sunward direction and northward or southward orientation of the interplanetary magnetic field (IMF) [8, 10, 2]. Probably as a result of reconnection events within Mercury's magnetosphere, large portions of the nightside are regularly bombarded by energetic particles [11, 12, 2]. During orbital operations, the XRS has detected energetic elections [13] and electron-induced X-ray fluorescence from Mercury's nighttime surface, confirming the precipitation of electrons to the surface [14]. Variations of ion and electron flux with latitude are strongly influenced by the north-south asymmetry in Mercury's internal field [15], in addition to the IMF configuration. Figure 2 shows the variation in precipitation with latitude for a northward IMF configuration, including the internal field asymmetry. With these plots Mercury's surface can be divided into latitude regions of varying particle flux.

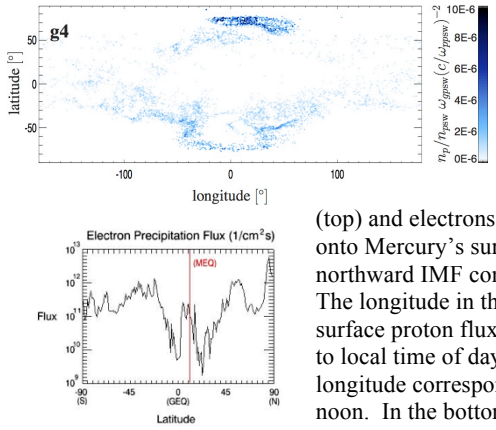

Fig. 2. Results from global hybrid simulations [8,10] of the flux of protons (top) and electrons (bottom) onto Mercury's surface for a northward IMF configuration. The longitude in the plot of surface proton flux corresponds to local time of day, and 0° longitude corresponds to local noon. In the bottom panel MEQ denotes the location of Mercury's magnetic equator.

Regional Variability. We have examined Mercury's spectral and elemental abundance properties in the context of the temperature-defined longitudinal sectors and the particle-precipitation-defined latitude bands. We included MDIS-derived color properties, MASCS VNIR observations, and elemental abundances for Mg, K, Na, and Fe measured by the GRNS and XRS [16–19]. With a geological map of Mercury [20], we selected three geologic units for sampling: intercrater plains (IcP), smooth plains (SP), and bright ejecta deposits (BE).

These three geologic units represent three distinct ranges in surface age. The IcP, with the highest impact crater densities, are considered the oldest. The SP are intermediate in age, and crater size-frequency distributions are consistent with their formation shortly after cessation of the late heavy bombardment [20–26]. The third unit, BE, consists of recently excavated deposits that are among the youngest materials on Mercury.

Preliminary analysis of the MDIS color, MASCS spectral, and elemental composition data show correlations with geological unit. MDIS data do not vary with latitude or longitude. MASCS data reveal possible latitude trends but no clear correlations with longitude. These results support a tentative conclusion that ion flux is more important than thermal factors in Mercury's space weathering. Better statistical sampling and analysis is critical. Confirmation of these results with a larger sample set would determine if Mercury's surface has nearly reached an end-member, stable, alteration state.

Maps of elemental abundance show a chemically heterogeneous surface, and the composition is often, but not always, correlated with geologic unit [16–19]. Analysis of MASCS data shows, however, that some of Mercury's spectral characteristics do not correlate with geologic unit [23, 24]. Further analyses of compositional data sets (MASCS, XRS, GRNS) are needed to explore spatial correlations and further define the role of surface modification via space weathering on Mercury.

References. [1] Hendrix, A.R. and F. Vilas (2006) *Astron. J.* 132, 1396. [2] Domingue, D.L. et al. (2014), *Space Sci. Rev.*, in press. [3] Helbert, J. et al (2013), *Earth Planet. Sci. Lett*. 369, 233. [4] Helbert, J. and A. Maturilli (2009), *Earth Planet. Sci. Lett*. 285, 347. [5] Jones, J. and P. Brown, (1993) *Mon. Not. Roy. Astron. Soc*. 265, 524. [6] Taylor, A.D. (1997) *Adv. Space Res.* 20(8), 1505. [7] Janches, D. et al. (2006) *J. Geophys. Res.* 111, A07317. [8] Schriver, D. et al. (2011) *Planet. Space Sci*. 59, 2026. [9] Vasavada, A.R. et al. (1999) *Icarus* 141, 179. [10] Schriver, D. et al. (2011) *Geophys. Res. Lett.* 38, L23103. [11] Slavin, J.A. et al. (2010) *Geophys. Res. Lett*. 37, L02105. [12] Slavin, J.A. et al. (2010) *Science* 329, 665. [13] Ho, G.C. et al. (2011) *Science* 333, 1865. [14] Starr, R.D. et al. (2012) *J. Geophys. Res.* 117, E002L02. [15] Anderson, B.J. et al. (2011), *Science* 333, 1859. [16] Weider, S.Z. et al. (2012), *J. Geophys. Res.* 117, E00l04. [17] Peplowski, P.N. (2012), *J. Geophys. Res.* 117, E00l04. [18] Weider, S.Z. et al. (2013), *Icarus,* submitted. [19] Weider, S.Z. et al. (2014), *LPS* 45, submitted. [20] Denevi, B.W. et al. (2013) *J. Geophys. Res. Planets* 118, 891. [21] Strom, R.G. et al. (1975) *J. Geophys. Res.* 80, 2478. [22] Strom, R.G. et al. (2008) *Science* 321, 79. [23] Trask, N.J. and J.E. Guest (1975) *J. Geophys. Res*. 80, 2461. [24] Spudis, P.D. and J.E. Guest (1988) in *Mercury* (F. Vilas, C.R. Chapman, M.S. Matthews, Eds.) Univ. Arizona Press, pp. 118-164. [25] Denevi, B.W. et al. (2009) *Science* 324, 613. [26] Head, J.W. et al. (2011) *Science* 333, 1853. [27] Helbert, J. et al. (2013), *J. Geophys. Res. Planets*, submitted. [28] D'Amore et al. (2014), *LPS* 45, no. 1073.